Experimental Investigation of Near-limit Gaseous Detonations in Small Diameter Spiral Tubing

Wei Cao [a,b]*, Dayuan Gao [a], Hoi Dick Ng [c] and John H.S. Lee [b]

[a] Institute of Chemical Materials, China Academy of Engineering Physics, Mianyang, Sichuan, 621999, China
[b] Department of Mechanical Engineering, McGill University, Montreal, Quebec, H3A 0C3, Canada

[c] Department of Mechanical, Industrial and Aerospace Engineering, Concordia University, Montreal, Quebec, H3G 1M8, Canada

Colloquium: DETONATIONS, EXPLOSIONS, AND SUPERSONIC COMBUSTION

Total length of paper is 6085 words and method 1 was used.

- Main Text: 2548 words
- References: 350 words
- Table 1: 137 words
- Figure 1 with caption: 128 words
- Figure 2 with caption: 128 words
- Figure 3 with caption: 200 words
- Figure 4 with caption: 160 words
- Figure 5 with caption: 825 words
- Figure 6 with caption: 124 words
- Figure 7 with caption: 485 words
- Figure 8 with caption: 500 words
- Figure 9 with caption: 500 words

* Corresponding author.

Institute of Chemical Materials, China Academy of Engineering Physics, Mianyang, Sichuan, 621999, China. Tel:+86-8162485366, E-mail: weicao@caep.cn

Abstract

The near-limit propagation of gaseous detonations in seven explosive mixtures with different reaction sensitivities is investigated. Experiments were performed in transparent tubing of four different inner diameters with relatively long tubing length (l/d > 2500 except l/d > 1000 for the largest diameter) arranged in a spiral configuration. Up to 83 fiber optics spaced at regular intervals along the tube were used to provide high resolution velocity measurement. Up to 8 cycles of the galloping mode were recorded, and the spiral boundary did not influence the persistence of galloping detonations. Results confirm that for mixtures with increasing argon dilution, making the detonation more stable with regular cellular pattern, the occurrence of galloping detonation diminishes. For stable mixtures with sufficiently large amount of argon dilution (e.g., stoichiometric C_2H_2/O_2 with 70%Ar), the galloping mode was not observed in all tested tubing. For unstable mixtures, smaller diameters were necessary to achieve the galloping mode. The range of initial pressures, within which galloping detonations were observed decreases rapidly with increasing tubing diameter. These results suggest that both the instability and the boundary effect are essential for galloping detonations. From the velocity histogram and the probability distribution function, a bimodal behavior was also observed in all galloping regimes of different unstable mixtures, with dominant modes near half of the Chapman-Jouguet detonation velocity (D_{CJ}) and D_{CJ}. With decreasing pressure, the lower velocity mode became more prevalent until no more galloping detonation occurred. The normalized wavelength of the galloping cycle (L/d) ranges from 250 to 450 within experimental variation. Nevertheless, few results show a clear minor trend that the wavelength increases with decreasing initial pressure. By looking at the velocity amplitude in the galloping cycle, the lower value as well as the average is relatively constant, while the upper peak has larger fluctuations.

Keywords: gaseous detonation; near-limit propagation; galloping mode; spiral tubing; instability

1. Introduction

The behavior of near-limit gaseous detonations propagating in small tubes is very complex. As the detonation limits are approached, the steady detonation velocity decreases, typically to about 80–90% of the Chapman–Jouguet value D_{CJ} [1, 2]. Before failure, the detonation velocity often shows large longitudinal fluctuations, rendering the average velocity of doubtful significance [1]. Far from the limits, the frequency of the transverse instability is high (or equivalently the detonation cell size is small); As the initial pressure P_o decreases, the instability tends towards lower modes with increasing cell size, and eventually the multi-headed detonation changes to a single-head spin [3, 4]. Beside their fundamental importance on detonation theory, detonation limits are also critical for safety control in industries. Hence, experimental data on detonation limits have been measured extensively for many explosives in different geometrical configurations [5-8].

There are generally five modes of near-limit behavior in the sequence of decreasing P_o: stable, stuttering, galloping, fast flame and failure [9-11]. Of great interest is the galloping detonation where its dynamics exhibits a longitudinal instability involving failure and re-initiation. For the galloping mode, the detonation velocity falls close to $0.5D_{CJ}$, then accelerates to about $1.5D_{CJ}$ and subsequently decays again for the next galloping cycle [11-13]. However, not all gaseous mixtures exhibit the five modes near the limit. Gao *et al.* [13] summarized all the observations and reported that galloping detonations are not observed in highly argon-diluted mixtures and in relatively large diameter tubes. It appears that unstable mixtures - with irregular cellular detonation patterns - and small tube diameters are necessary conditions for galloping detonations.

The length of a galloping detonation cycle typically spans about 350 tube diameters, $L \sim 350d$. Due to insufficient observation lengths used in previous studies [4, 13], it remains inconclusive for some mixtures at low P_o, whether the detonation wave will fail or re-initiate again to develop into a galloping

detonation. Experiments with longer tube lengths have been recommended to further distinguish the boundary of existence and assess the characteristics of galloping detonations.

In Jackson *et al.* [9], a novel configuration was proposed to look at the near-limit detonations by using a transparent tube coiled in a spiral geometry. Such an arrangement has provided a sufficiently long observation length (l/d > 7300). Furthermore, the spiral geometry using flexible tubing does not appear to influence the wave dynamics from the comparison between results using the spiral and straight tubing. The use of this spiral geometry also recorded all near-limit detonation regimes and up to 20 persistent cycles of the galloping phenomenon. High-speed video with image processing was used to obtain high-temporal-resolution velocity measurement of the luminous front. Nevertheless, only one tube diameter of 4.1 mm and the stoichiometric propane-oxygen mixture was considered in [9].

Taking advantage of this spiral tube configuration, we perform in this work a parametric study to investigate the near-limit detonations of seven explosive mixtures with different reaction sensitivities. Experiments were conducted using transparent tubing of different diameters, d = 3.18, 6.35, 12.7 and 25.4 mm, with relatively long tubing length (l/d > 2500 except l/d > 1000 for the largest diameter). Wave velocities were obtained using regularly spaced photo fibers along the entire tube length. The observation length achieved by using the spiral configuration provides reliable quantitative data for the characterization of galloping detonations including the histograms and the probability distribution of velocity as well as the wavelength and amplitudes of the galloping cycle. The present results also distinguish unambiguously the required conditions for the existence of galloping detonations.

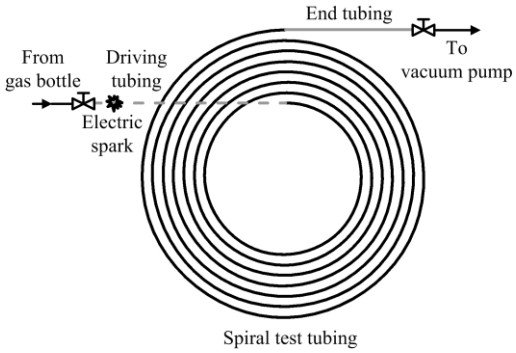

Fig. 1. The experimental setup.

Table 1. Parameters for different experimental apparatus configurations

Case no.	Test tubing				Driving tubing		
	Diameter d (mm)	Thickness δ (mm)	Normalized length l/d	Minimum spiral radius (m)	Diameter d (mm)	Thickness δ (mm)	Length l (m)
1	3.18	1.59	2583	0.5	12.7	3.18	0.5
2	6.35	1.59	2583	0.5	12.7	3.18	0.5
3	12.7	3.18	2583	0.5	12.7	3.18	0.5
4	25.4	6.35	1197	1	25.4	6.35	0.5

2. Experimental Details

The apparatus consists of small-diameter, transparent, polyvinyl chloride (PVC) tubing coiled in a spiral configuration. Figure 1 shows a schematic of the setup. Different configurations are detailed in Table 1. A detonation was initiated by a high-voltage spark discharge in the driving tubing. For low P_o and insensitive mixtures, C_2H_2+O_2 was used in the driving tubing to initiate the tested mixture. For the case with d = 25.4 mm, the normalized length l/d is about 1200, thus few galloping cycles may be observed. Nevertheless, this case is mainly for the verification purpose of previous observations.

Up to 83 2-mm-diameter optical fibers terminating in a photodiode were used and spaced every 10, 20, 40 and 40 cm, respectively for tubing with d = 3.18, 6.35, 12.7 and 25.4 mm (or a spacing of l/d = 31.5 for the first three diameters and l/d = 15.7 for d = 25.4 mm). Local wave velocity was deduced from the time-of-arrival at two neighboring optical probe locations. The NASA CEA program was used

to compute D_{CJ} for the various mixtures. For a given mixture and tube diameter, the detonation limits are approached by progressively lowering P_o.

For each experiment, the tubing was evacuated to at least 0.01 kPa and then filled with the mixture to the desired P_o. The pressure was monitored by Omega transducers model PX309-200AI for high pressure (0~1379 kPa) and PX309-005AI for low pressure (0~34.5 kPa) both with an accuracy of ±0.25% full scale. Five stoichiometric mixtures: CH_4+2O_2, $C_3H_8+5O_2$, $C_2H_2+5N_2O$, $C_2H_2+2.5O_2+50\%Ar$ and $C_2H_2+2.5O_2+70\%Ar$, and two off-stoichiometric mixtures: $C_3H_8+2.5O_2$ (φ = 2) and $C_3H_8+10O_2$ (φ = 0.5), were tested. These were premixed via partial pressure in separate mixing bottles and were allowed to mix by diffusion for at least 24 hrs before testing. Note that these mixtures provide different degrees of detonation instability, which can be illustrated using the stability parameter χ defined as $\chi = \frac{E_I}{T_S}\frac{\Delta_I}{\Delta_R}$, where E_I is the global activation energy describing the sensitivity of the thermally neutral chemical induction process, T_s is the post-shock temperature. Δ_I and Δ_R denote the characteristic induction and reaction length, respectively (see [14] for more details). The χ values of the different mixtures are given in Fig. 2. The mixture with the highest χ value, i.e., CH_4+2O_2, represents the most unstable mixture used in this investigation.

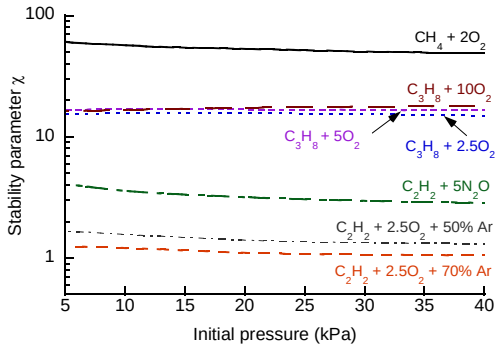

Fig. 2. The stability parameter χ for different mixtures.

3. Results and Discussions

Figure 3 presents the average detonation velocity data for the stoichiometric CH_4+$2O_2$ and C_3H_8+$5O_2$ mixtures. As in [9], these plots nearly collapse all data to one curve by showing the normalized wave velocity D/D_{CJ} as a function of the binary scaling parameter $1/(P_o d)$. Similar results were obtained for all other tested mixtures, see *Supplementary Materials*. Figure 4 summarizes the conditions under which galloping detonations could be observed from the present results. For unstable mixtures (e.g., CH_4+$2O_2$, C_3H_8+$5O_2$, C_2H_2+$5N_2O$, C_2H_2+$2.5O_2$+50%Ar), galloping detonations were observed in small diameter tubes (d = 3.18 and 6.35 mm). For few cases, the galloping mode disappears at d = 12.7 mm and only for the highly unstable CH_4+O_2 mixture could a galloping detonation be sustained at d = 25.4 mm within a very narrow condition. With the presence of galloping mode and other irregular velocity fluctuations in unstable mixtures, the average velocity can reach as low as 0.5–0.6D_{CJ} before the detonation wave fails. In contrast, for the stable mixture (C_2H_2+$2.5O_2$+70%Ar) and few unstable mixtures in large diameter tubing (e.g., C_2H_2+$2.5O_2$+50%Ar and C_3H_8+$2.5O_2$, d = 12.7 mm), no galloping detonation was observed, and the average detonation velocity drops only to ~0.8D_{CJ} before the detonation fails.

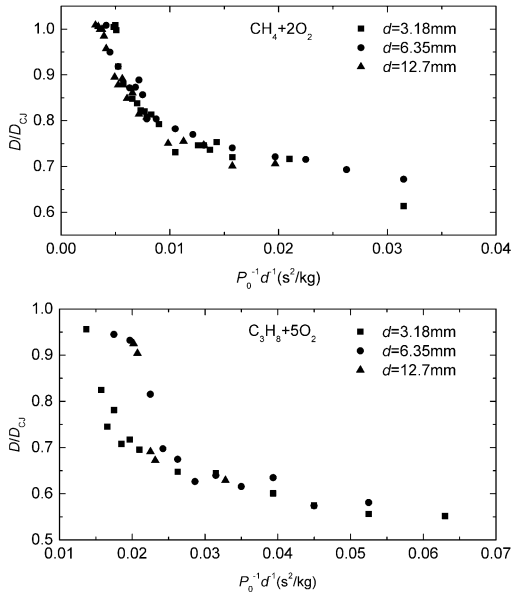

Fig. 3. Average velocity data for CH_4+$2O_2$ and C_3H_8+$5O_2$.

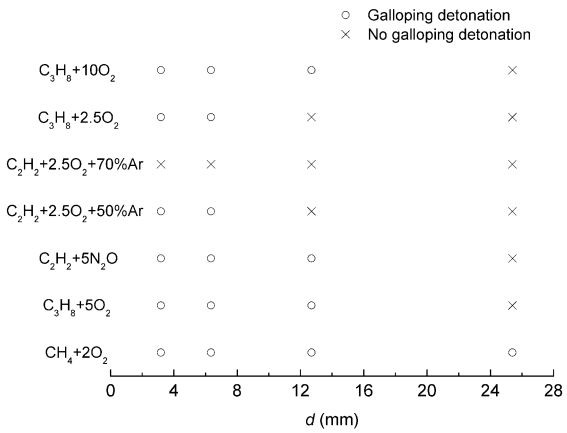

Fig. 4. Mixture conditions for galloping detonation.

The fact that galloping detonations are only observed in small diameter tubing for unstable mixtures indicates that both instability and small diameter tube boundary are necessary for producing galloping detonations. The boundary layer growth in small diameter tubes where significant unburned shocked reactant leaks through, together with transverse acoustic disturbances continuously amplifying by their frequency of interaction with the tube wall and the high temperature sensitivity of the unstable mixture, leads to the onset of an explosion to re-initiate an overdriven detonation for the next galloping cycle. The repeatable oscillatory behavior of galloping detonation thus relies on the strong coupling between the gasdynamic processes and sensitivity of the chemical reactions.

To elucidate different behaviors of near-limit detonations, Fig. 5 shows a series of local velocity variation with normalized length (l/d) and its histogram in order of decreasing initial pressure P_o for CH_4+2O_2 and d = 3.18 mm (see *Supplementary Materials* for additional illustrations). The histograms provide essentially information on the relative frequency or probability distribution of each velocity present in the variation with the raw data binned in $0.1D_{CJ}$ bin width [9, 10]. Far above the limit, a steady propagation can be seen with the velocity histogram peaking at D_{CJ}. When P_o decreases towards the limit, the local velocity fluctuates. For the stuttering regime, a broader velocity distribution can be seen in the histogram while the dominant velocity mode is still around D_{CJ}. For further decrease in P_o

the galloping behavior of the detonation appears. In the galloping regime, bimodal behavior with dominant velocity modes of about $0.6D_{CJ}$ and D_{CJ} are also observed as in the previous study [9]. The galloping mode is regular and repeatable for up to 8 cycles. With decreasing P_o, the lower velocity mode becomes more prevalent as shown in the histogram where probability of the D_{CJ} mode shifts toward the lower velocity range until no more galloping detonation occurs. Past the galloping regime, the velocity modes distribute around $0.6\sim0.8D_{CJ}$, the fast flame or low-velocity detonation regime [15]. The appearance of velocity fluctuations in both stuttering and fast flame regimes is found to be random along the propagation path.

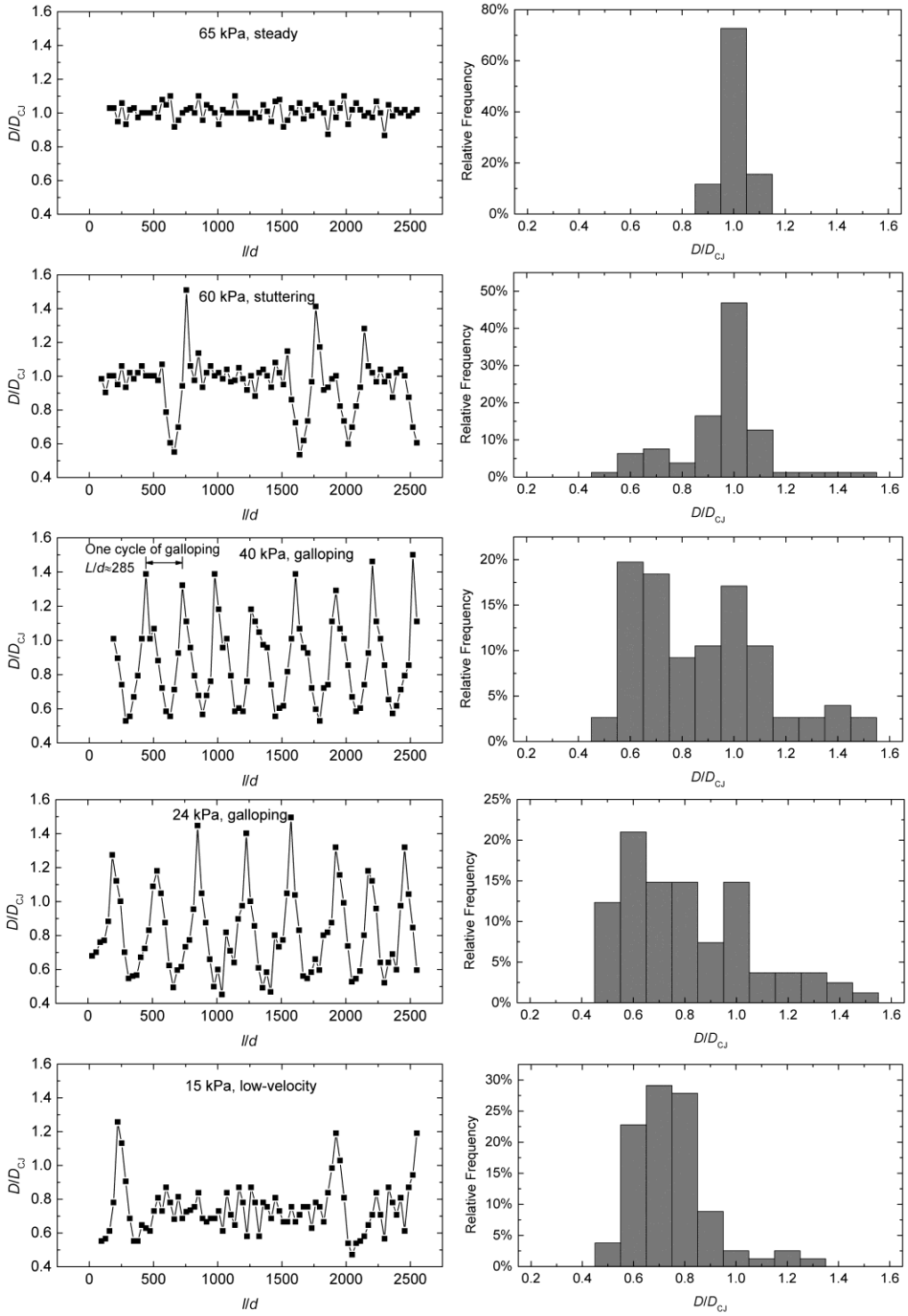

Fig. 5. Normalized velocity and histograms of CH_4+2O_2 with d = 3.18 mm at different P_o.

All observed velocity modes can be better represented by the probability distribution function (PDF) computed using linear interpolation of each histogram data in both P_o and D/D_{CJ} with the relative

frequencies from the D/D_{CJ} data binned in 0.1 increments [9]. A PDF map in both the P_o and D/D_{CJ} dimensions is shown in Fig. 6 for CH_4+$2O_2$ with d = 3.18 mm (see *Supplementary Materials* for additional cases). Above P_o > 55 kPa, a single peak can be clearly seen. The bimodal velocity distribution with peaks around 0.6 D_{CJ} and D_{CJ} in the galloping regime occurs from P_o = 30 to 55 kPa. The prevalent shift toward the lower velocity mode with decreasing P_o within the galloping regime can be observed from the PDF. At low initial pressures, P_o < 38 kPa, the low velocity mode has a higher probability mapping the fast flame regime. Similar PDFs are also obtained for other unstable mixtures having the galloping regime. These results are in agreement with [9].

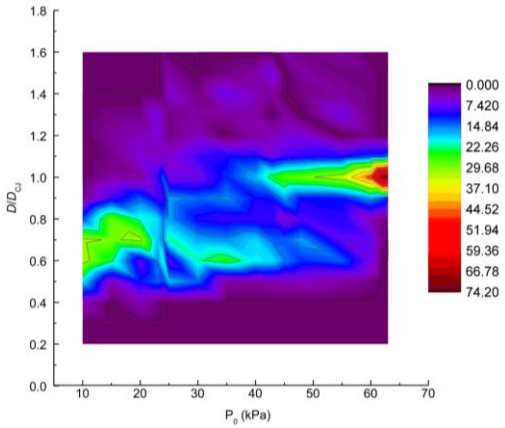

Fig. 6. Velocity PDF with varying P_o for CH_4+$2O_2$ with d = 3.18 mm.

To assess the galloping detonation characteristics, the interval of initial pressure and its width $\Delta P = P_U - P_L$ (where P_U is the upper limit when galloping detonations first appear and P_L is the lower limit where galloping detonations last appear) are shown in Fig. 7 (and Fig. S8a in *Supplementary Materials*). It is evident from these plots that the range of ΔP depends on the mixture sensitivity and tube diameter. For mixtures with very high degree of instability (e.g., CH_4+$2O_2$ or C_3H_8+$5O_2$), the galloping detonation exists over a larger span of initial pressure. This is consistent with the off-stoichiometric propane-oxygen mixtures where the lean side shows a wider existence range of galloping detonation due to its

higher degree of instability compared to the rich condition. For all cases, ΔP decreases rapidly as the tubing diameter increases. For fuel-rich C_3H_8+2.5O_2 (also C_2H_2+2.5O_2+50%Ar in *Supplementary Materials*), $\Delta P \rightarrow 0$ for d = 12.7 mm and galloping detonations were not observed. Further experiments using the largest tube diameter d = 25.4 mm have verified that no galloping detonation was observed for C_3H_8+5O_2, C_2H_2+5N_2O and C_3H_8+10O_2, and galloping detonation occurs only for CH_4+2O_2 within a narrow range of initial pressure (ΔP = 4.5–3.5 = 1 kPa). In the literature, the criterion λ/d = 2 or π for the onset of single-head spinning detonations has long been proposed [2], where λ is the detonation cell size [16]. The λ/d of the upper pressure limit is also indicated in Fig. 7 (and Fig. S8a). The present results exhibit galloping onset at some value between λ/d =1.9 and 4.3 for different unstable mixtures, just past the single-head spinning detonation for most cases.

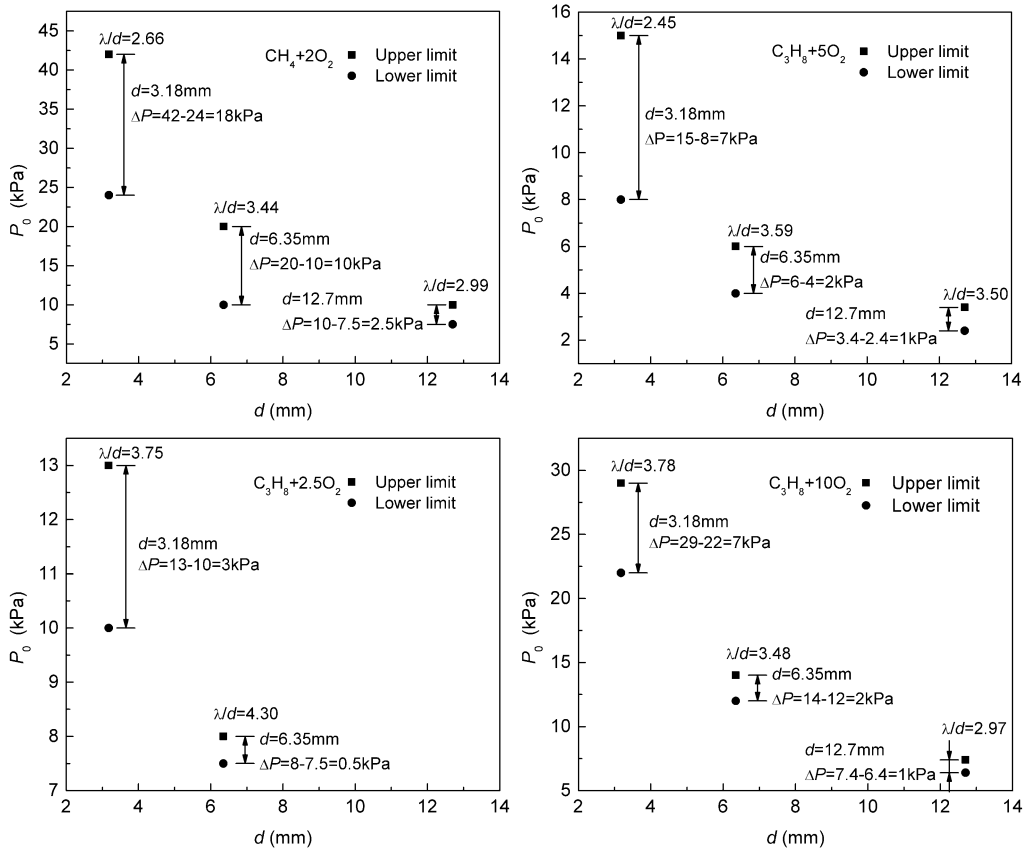

Fig. 7. Upper and lower pressure limits of galloping detonation as a function of tube diameter.

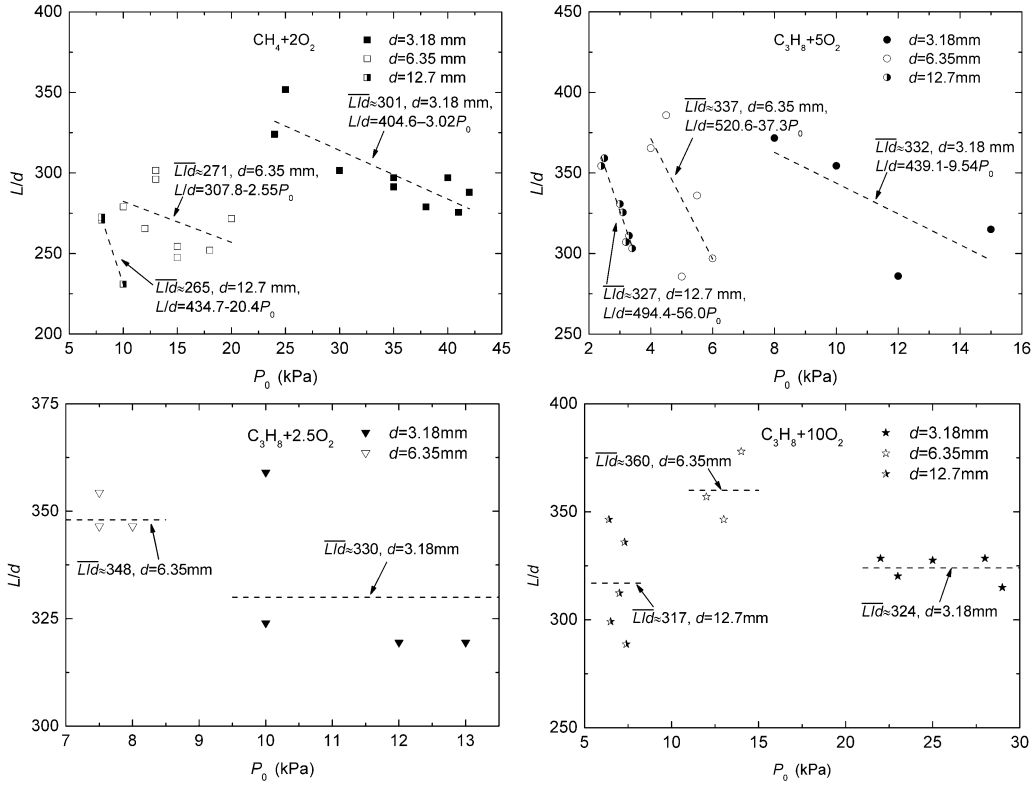

Fig. 8. Galloping wavelength as a function of initial pressure.

Figure 8 shows the normalized wavelength L/d of the galloping cycle as defined in Fig. 5 for four sample unstable mixtures with different tube diameters. The data in Fig. 8 was determined using several (5~8) galloping cycles. In agreement with other available data [13], the average $\overline{L/d}$ of all cases is about 350. The galloping wavelength has a moderately decreasing trend as P_o increases for each tube diameter as shown by a simple linear fit with negative slope. For the non-stoichiometric mixtures, this negative slope linear relationship is rather ambiguous and, the average wavelength line is thus simply drawn in Fig. 8.

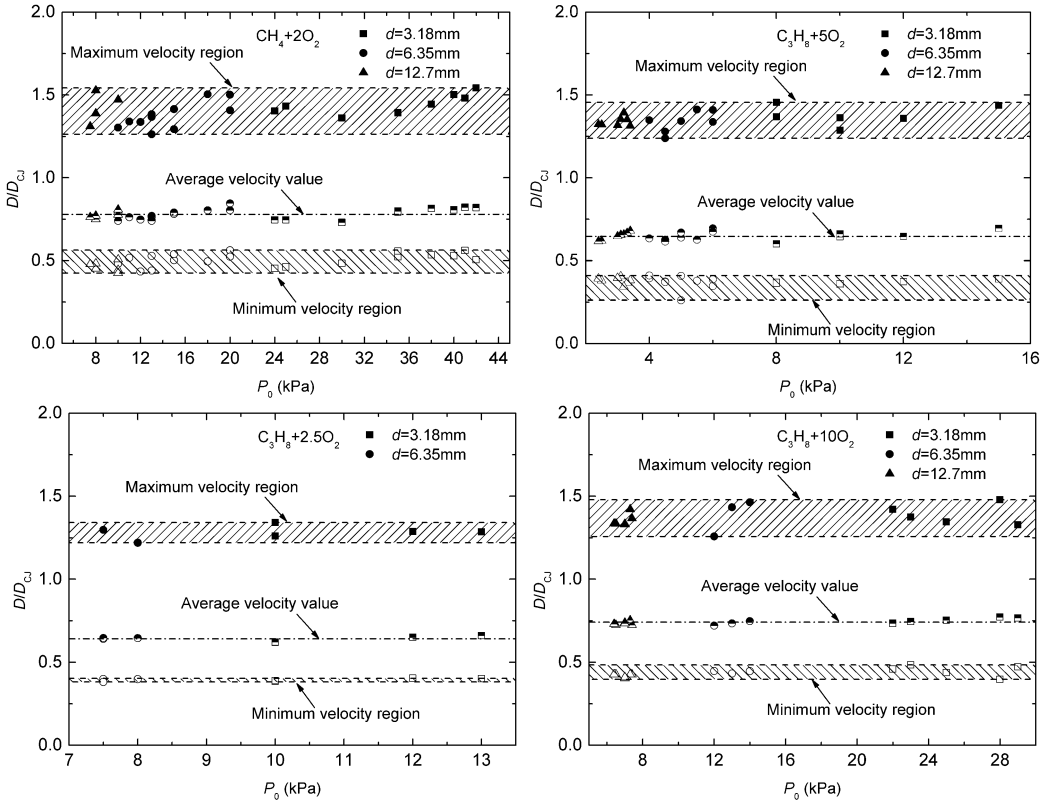

Fig. 9. Extrema and averaged velocity of galloping cycle.

The amplitude of the velocity fluctuation in an oscillatory cycle provides another important characteristic of the galloping detonation. Figure 9 shows the upper and lower velocity values in a galloping cycle for the same four unstable mixtures as a function of the initial pressure range within each galloping regime. The three (shaded) regions identify the range of maximum peak, average and minimum value of the galloping cycle(s). From these plots, one can see that the lower velocity mode and the average value are relatively constant, while the upper velocity exhibits a larger amplitude.

4. Conclusion

This investigation improves upon inconclusive findings on the existence of different near-limit detonation propagation modes in our previous works [4, 13]. To address the limitation in tube length, a spiral tube configuration with different diameters as proposed by Jackson et al. [9] is used to achieve a

much longer propagation distance (l/d > 2500 except l/d > 1000 for the largest diameter). The contribution of this work is the new results of using a variety of detonable mixtures, including stoichiometric and non-stoichiometric mixtures to carefully observe the near-limit detonation behavior. Different velocity modes are recorded from the local velocity variations and their corresponding histograms, and summarized using the probability distribution function.

The present results conclude that both the mixture sensitivity and the small boundary effect are vital for producing galloping detonations. For highly stable mixtures (e.g., C_2H_2+2.5O_2+70%Ar) or unstable mixtures where the tube diameter is large (e.g., above d > 12.7 mm except CH_4+2O_2 due its high degree of instability), no galloping detonation is observed and the velocity deficit drops to about ~0.8 D_{CJ} before detonation failure. The galloping behavior is described by two dominant velocity modes near half D_{CJ} and D_{CJ}. The lower velocity mode becomes more prevalent with decreasing pressure in the galloping regime. Past the galloping regime, the propagation mode is predominantly at the lower velocity range indicating a fast flame or a low-velocity detonation.

The range of P_o within which galloping detonations exist shrinks rapidly with tube diameter. The onset of galloping regime is also shown to pass the onset of single-head spinning detonation. In agreement with [13], the average wavelength $\overline{L/d}$ of the galloping cycle for all tested mixtures is ~350 and a minor trend is seen in few cases that L/d decreases with increasing P_o. Through galloping cycles, variations in the average and lower velocity, for different P_o, are small, while the peak velocity exhibits relatively larger fluctuations.

This paper aims to present a large amount of useful data that will expand the community's knowledge base on near-limit detonations. Further work is necessary to quantitatively analyze this trove of data, to achieve a rigorous model for near-limit detonation behaviors. The interaction between the reactive wave and boundary layer, other wall effects [17, 18] and the instabilities should be thoroughly considered to elucidate the near-limit detonation propagation mechanism.

Acknowledgments

This research is supported by the National Natural Science Foundation of China (11602238, 11572359), the China Scholarship Council (201604890002) and the Natural Sciences and Engineering Research Council of Canada (NSERC).

References

1. J.H.S. Lee, A. Jesuthasan, H.D. Ng, Proc. Combust. Inst. 34 (2) (2013) 1957-1963.
2. Y. Gao, H.D. Ng, J.H.S. Lee, Shock Waves 24 (2014) 447-454.
3. A.A. Vasil'ev, Shock Waves 18 (2008) 245-253.
4. Y. Gao, J.H.S. Lee, H.D. Ng, Combust. Flame 161 (2014) 2982-2990.
5. B. Zhang, X. Shen, L. Pang, Y. Gao, Fuel 177 (2016) 1-7.
6. S. Kitano, M. Fukao, A. Susa, N. Tsuboi, A.K. Hayashi, M. Koshi, Proc. Combust. Inst. 32 (2009) 2355–2362.
7. K. Ishii, M. Monwar, Proc. Combust. Inst. 33 (2011) 2359–2366.
8. K Yoshida, K Hayashi, Y Morii, N Tsuboi, AK Hayashi, Combut. Sci. Tech. 188 (11-12) (2016) 2012-2025.
9. S. Jackson, B.J. Lee, J.E. Shepherd, Combust. Flame 167 (2016) 24-38.
10. J.J. Lee, G. Dupré, R. Knystautas, J.H.S. Lee, Shock Waves 5 (1995) 175-181.
11. F. Haloua, M. Brouillette, V. Lienhart, G. Dupré, Combust. Flame 122 (2000) 422-438.
12. K. Ishii, H. Gronig, Shock Waves 8 (1998) 55-61.
13. Y. Gao, H.D. Ng, J.H.S. Lee, Combust. Flame 162 (2015) 2405-2413.
14. H. D. Ng, M. I. Radulescu, A. J. Higgins, N. Nikiforakis, J. H. S. Lee, Combust. Theory Model. 9 (3) (2005) 385-401.
15. V. Manzhalei, Combust. Expl. Shock Waves 35 (3) (1999) 296-302.

16. M. Kaneshige, J.E. Shepherd, Detonation Database, Report No. FM97-8, Graduate Aeronautical Laboratories, California Institute of Technology, 1997.
17. R.W. Houim, A. Ozgen, E.S. Oran, Combust. Theory Model. 20 (6) (2016) 1068-1087.
18. W. Han, Y. Gao, C.K. Law, Combust. Flame 176 (2017) 285-298.

Table Caption

Table 1. Parameters for different experimental apparatus configurations

Case no.	Test tubing				Driving tubing		
	Diameter d (mm)	Thickness δ (mm)	Normalized length l/d	Minimum spiral radius (m)	Diameter d (mm)	Thickness δ (mm)	Length l (m)
1	3.18	1.59	2583	0.5	12.7	3.18	0.5
2	6.35	1.59	2583	0.5	12.7	3.18	0.5
3	12.7	3.18	2583	0.5	12.7	3.18	0.5
4	25.4	6.35	1197	1	25.4	6.35	0.5

Table 1.

Figure Captions

Fig.1. The experimental setup.

Fig. 2. The stability parameter χ for different mixtures.

Fig. 3. Average velocity data for CH_4+2O_2 and $C_3H_8+5O_2$.

Fig. 4. Mixture conditions for galloping detonation.

Fig. 5. Normalized velocity and histograms of CH_4+2O_2 with d = 3.18 mm at different P_o.

Fig. 6. Velocity PDF with varying P_o for CH_4+2O_2 with d = 3.18 mm.

Fig. 7. Upper and lower pressure limits of galloping detonation as a function of tube diameter.

Fig. 8. Galloping wavelength as a function of initial pressure.

Fig. 9. Extrema and averaged velocity of galloping cycle.

Supplementary Materials

Figure Captions

Fig. S1. Average velocity data versus inverse binary scaling parameter ($1/P_o d$) for C_2H_2+5N_2O, C_2H_2+2.5O_2+50% Ar, C_2H_2+2.5O_2+70% Ar, C_3H_8+2.5O_2 and C_3H_8+10O_2.

Fig. S2. Normalized velocity and histograms of C_3H_8+10O_2 at different P_o with d = 3.18 mm.

Fig. S3. PDF of the velocity with initial mixture pressure for C_3H_8+10O_2 with d = 3.18 mm.

Fig. S4. Normalized velocity and histograms for C_3H_8+2.5O_2 at different P_o with d = 3.18 mm.

Fig. S5. PDF of the velocity with initial mixture pressure for C_3H_8+2.5O_2 with d = 3.18 mm.

Fig. S6. Normalized velocity and histograms for C_2H_2+5N_2O at different P_o with d = 6.35 mm.

Fig. S7. PDF of the velocity with initial mixture pressure for C_2H_2+5N_2O with d = 6.35 mm.

Fig. S8. a) Upper and lower pressure limits of galloping detonation as a function of tubing diameter; b) Galloping wavelength as a function of initial pressure; and c) Extrema and averaged velocity of galloping cycle for C_2H_2+5N_2O and C_2H_2+5O_2+50%Ar mixtures

Table Captions

Table S1. Test data summary for d = 3.18 mm.

Table S2. Test data summary for d = 6.35 mm.

Table S3. Test data summary for d = 12.7 mm.

Table

Case no.	Test tubing				Driving tubing		
	Diameter d (mm)	Thickness δ (mm)	Normalized length l/d	Minimum spiral radius (m)	Diameter d (mm)	Thickness δ (mm)	Length l (m)
1	3.18	1.59	2583	0.5	12.7	3.18	0.5
2	6.35	1.59	2583	0.5	12.7	3.18	0.5
3	12.7	3.18	2583	0.5	12.7	3.18	0.5
4	25.4	6.35	1197	1	25.4	6.35	0.5

Table 1.

Figure

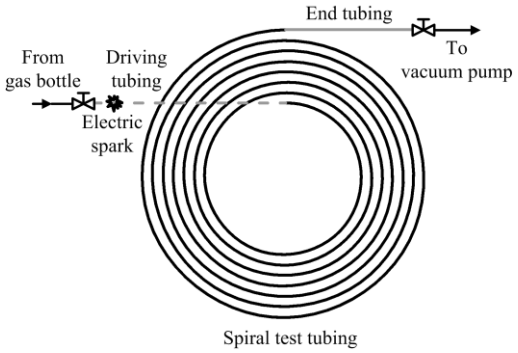
End tubing
To
vacuum pump
From
gas bottle
Driving
tubing
Electric
spark
Spiral test tubing

Fig. 1.

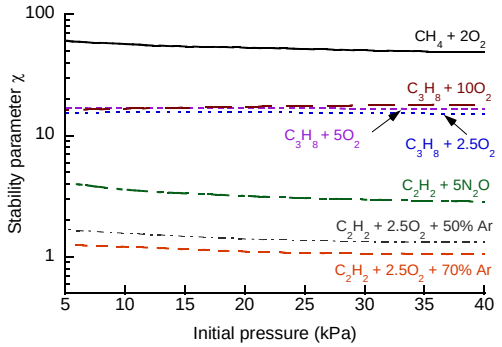
100
10
1
Stability parameter χ
5
10
15
20
25
30
35
40
Initial pressure (kPa)
CH4 + 2O2
C3H8 + 10O2
C3H8 + 5O2
C3H8 + 2.5O2
C2H2 + 5N2O
C2H2 + 2.5O2 + 50% Ar
C2H2 + 2.5O2 + 70% Ar

Fig. 2.

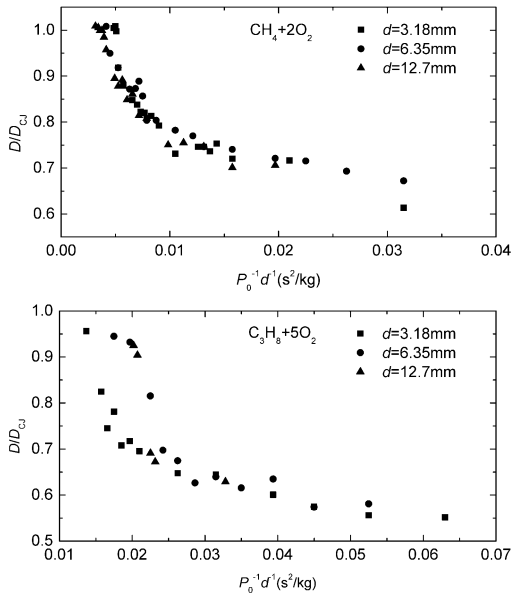
CH4+2O2
d=3.18mm
d=6.35mm
d=12.7mm
D/DCJ
P0-1d-1(s2/kg)
C3H8+5O2
d=3.18mm
d=6.35mm
d=12.7mm
D/DCJ
P0-1d-1(s2/kg)

Fig. 3.

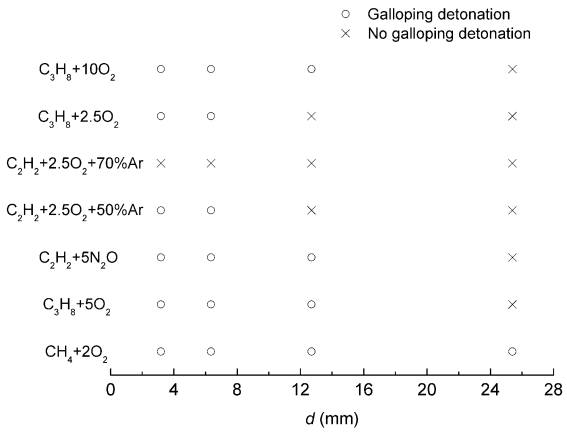
○ Galloping detonation
× No galloping detonation
C3H6+10O2
C3H8+2.5O2
C2H2+2.5O2+70%Ar
C2H2+2.5O2+50%Ar
C2H2+5N2O
C3H8+5O2
CH4+2O2
0
4
8
12
16
20
24
28
d (mm)

Fig. 4.

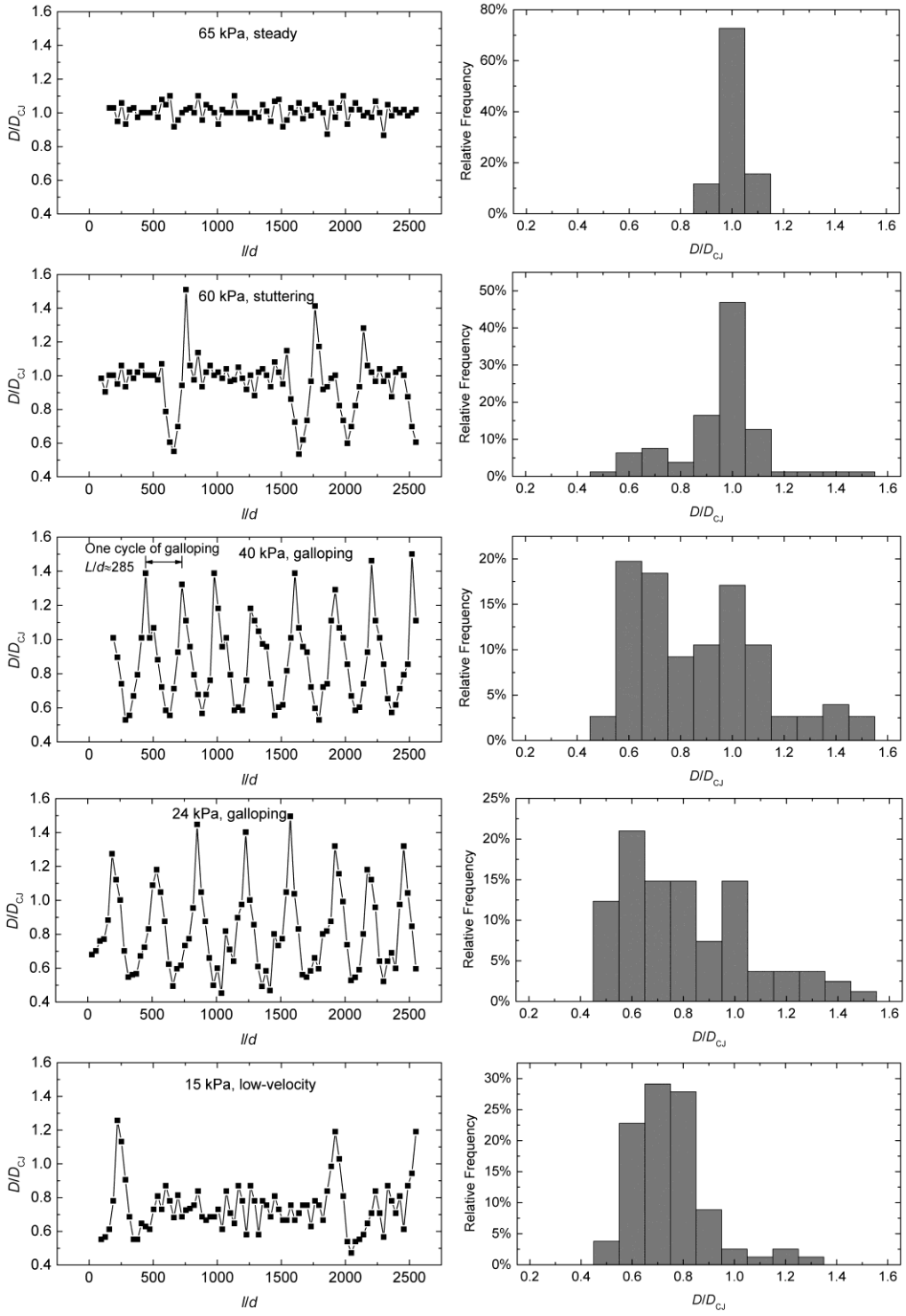
65 kPa, steady
60 kPa, stuttering
One cycle of galloping
L/d≈285
40 kPa, galloping
24 kPa, galloping
15 kPa, low-velocity
D/D_CJ
l/d
Relative Frequency

Fig. 5.

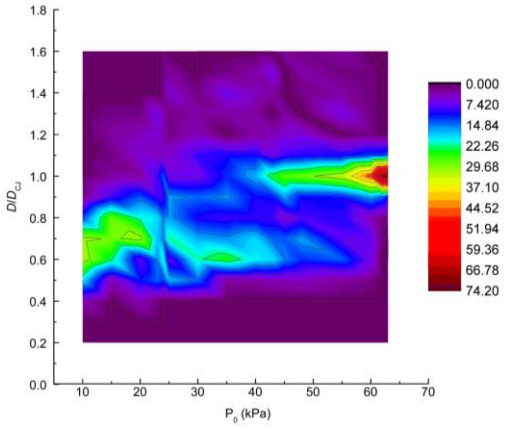
1.8
1.6
1.4
1.2
1.0
0.8
0.6
0.4
0.2
0.0
D/D_cj
10
20
30
40
50
60
70
P_0 (kPa)
0.000
7.420
14.84
22.26
29.68
37.10
44.52
51.94
59.36
66.78
74.20

Fig. 6.

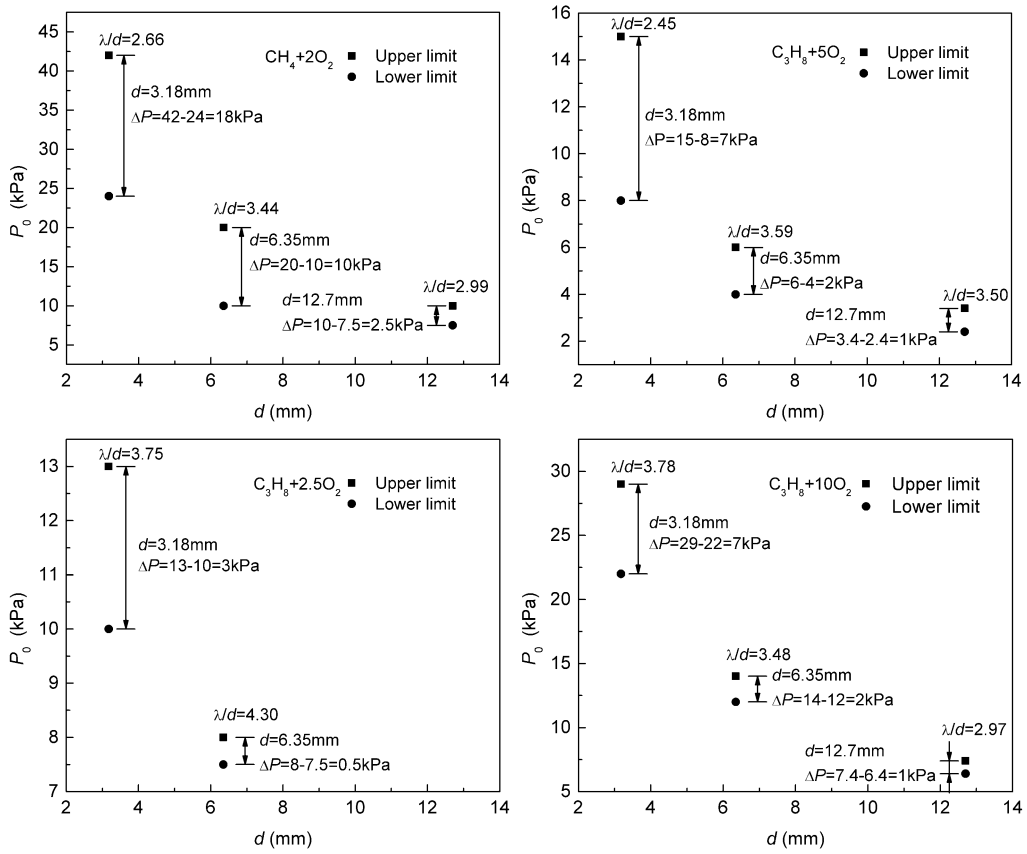
λ/d=2.66
CH4+2O2
Upper limit
Lower limit
d=3.18mm
ΔP=42-24=18kPa
λ/d=3.44
d=6.35mm
ΔP=20-10=10kPa
d=12.7mm
ΔP=10-7.5=2.5kPa
λ/d=2.99
P0 (kPa)
d (mm)
λ/d=2.45
C3H8+5O2
Upper limit
Lower limit
d=3.18mm
ΔP=15-8=7kPa
λ/d=3.59
d=6.35mm
ΔP=6-4=2kPa
d=12.7mm
ΔP=3.4-2.4=1kPa
λ/d=3.50
P0 (kPa)
d (mm)
λ/d=3.75
C3H8+2.5O2
Upper limit
Lower limit
d=3.18mm
ΔP=13-10=3kPa
λ/d=4.30
d=6.35mm
ΔP=8-7.5=0.5kPa
P0 (kPa)
d (mm)
λ/d=3.78
C3H8+10O2
Upper limit
Lower limit
d=3.18mm
ΔP=29-22=7kPa
λ/d=3.48
d=6.35mm
ΔP=14-12=2kPa
d=12.7mm
ΔP=7.4-6.4=1kPa
λ/d=2.97
P0 (kPa)
d (mm)

Fig. 7.

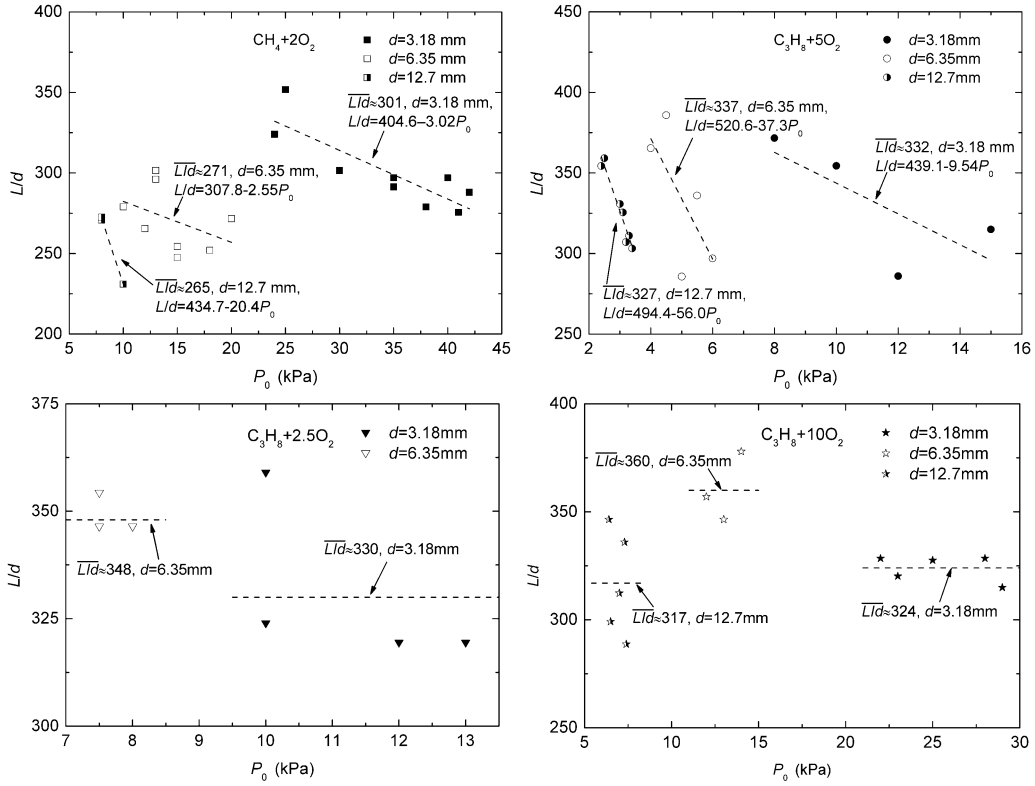
CH4+2O2
d=3.18 mm
d=6.35 mm
d=12.7 mm
L/d≈301, d=3.18 mm,
L/d=404.6–3.02P0
L/d≈271, d=6.35 mm,
L/d=307.8-2.55P0
L/d≈265, d=12.7 mm,
L/d=434.7-20.4P0
C3H8+5O2
d=3.18mm
d=6.35mm
d=12.7mm
L/d≈337, d=6.35 mm,
L/d=520.6-37.3P0
L/d≈332, d=3.18 mm
L/d=439.1-9.54P0
L/d≈327, d=12.7 mm,
L/d=494.4-56.0P0
C3H8+2.5O2
d=3.18mm
d=6.35mm
L/d≈330, d=3.18mm
L/d≈348, d=6.35mm
C3H8+10O2
d=3.18mm
d=6.35mm
d=12.7mm
L/d≈360, d=6.35mm
L/d≈317, d=12.7mm
L/d≈324, d=3.18mm
L/d
P0 (kPa)

Fig. 8.

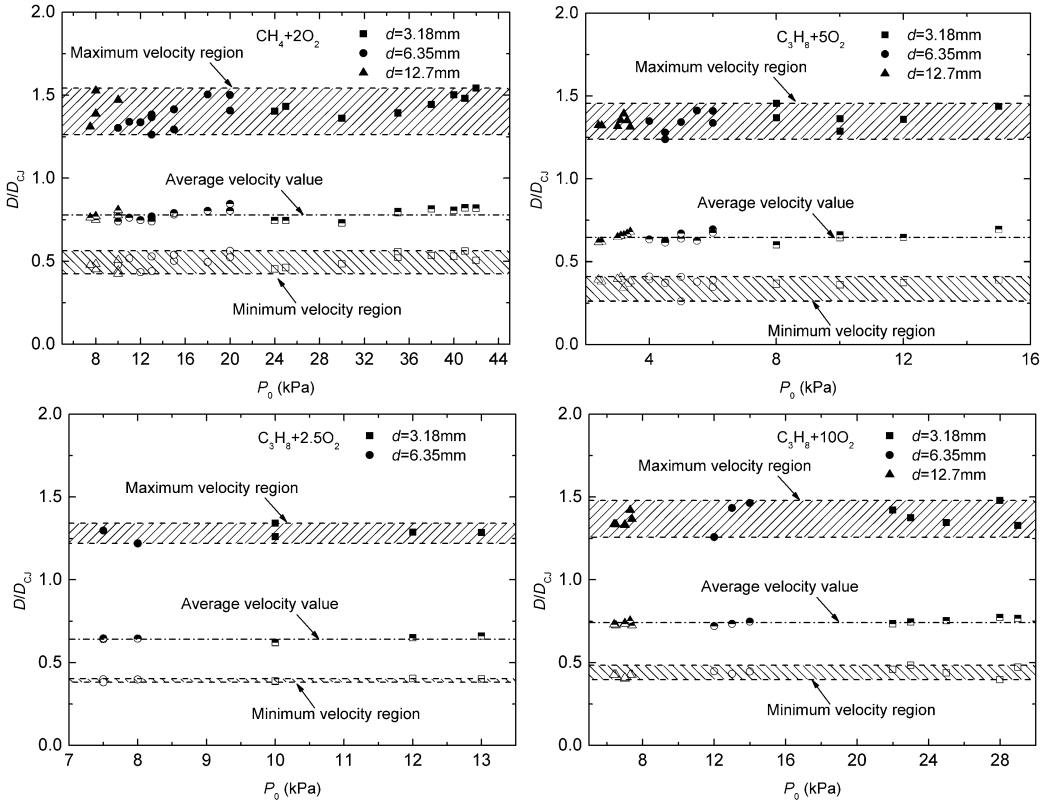
CH4+2O2
d=3.18mm
d=6.35mm
d=12.7mm
Maximum velocity region
Average velocity value
Minimum velocity region
D/DCJ
P0 (kPa)
C3H8+5O2
C3H8+2.5O2
C3H8+10O2

Fig. 9.

Supplemental Material

Click here to download Supplemental Material: Supplementary Material.docx

Supplemental Material (PDF version)

Click here to download Supplemental Material: Supplementary Material PDF version.pdf